Transforming growth factor-β signal regulates gut bending in the sea urchin embryo

doi: 10.1111/dgd.12434

Development, Growth & Differentiation
The Japanese Society of Developmental Biologists

TGF-ß signal regulates gut bending in the sea urchin embryo

Journal:	*Development Growth and Differentiation*
Manuscript ID	DGD-00015-2018.R1
Manuscript Type:	Original Research Article
Date Submitted by the Author:	n/a
Complete List of Authors:	Suzuki, Haruka; University of Tsukuba, Shimoda Marine Research Center Yaguchi, Shunsuke; University of Tsukuba, Shimoda Marine Research Center
Key Words:	gastrulation, morphogenesis, Nodal, Smad

TGF-ß signal regulates gut bending in the sea urchin embryo

Haruka Suzuki, Shunsuke Yaguchi*

Shimoda Marine Research Center, University of Tsukuba, 5-10-1 Shimoda, Shizuoka 415-0025, Japan

Running title: TGF-ß bends the gut.

Keywords: Nodal, morphogenesis, ventral, dorsal, SB431542

*Corresponding Author: Shunsuke Yaguchi, Shimoda Marine Research Center, University of Tsukuba, 5-10-1, Shimoda, Shizuoka, Japan 415-0025

Phone: +81-558-22-6716

Fax: +81-558-22-0346

E-mail: yag@shimoda.tsukuba.ac.jp

ORCID: 0000-0002-8326-5762

Abstract

During gastrulation, one of the most important morphogenetic events in sea urchin embryogenesis, the gut bends toward the ventral side to form an open mouth. Although the involvement of TGF-ß signals in the cell-fate specification of the ectoderm and endoderm along the dorsal-ventral axis has been well reported, it remains unclear what controls the morphogenetic behavior of gut bending. Here, using two sea urchin species, *Hemicentrotus pulcherrimus* and *Temnopleurus reevesii*, we show that TGF-ß signals are required for gut bending toward the ventral side. To search for the common morphogenetic cue in these two species, we initially confirmed the expression patterns of the dorsal-ventral regulatory TGF-ß members nodal, lefty, bmp2/4, and chordin in *T. reevesii* because these factors are appropriate candidates to investigate the cue that starts gut bending, although genetic information about the body axes is entirely lacking in this species. Based on their expression patterns and a functional analysis of Nodal, the dorsal-ventral axis formation of *T. reevesii* is likely regulated by these TGF-ß members, as in other sea urchins. When the Alk4/5/7 signal was inhibited by its specific inhibitor, SB431542, before the late gastrula stage of *T. reevesii*, the gut was extended straight toward the anterior tip region, although the ectodermal dorsal-ventral polarity was normal. By contrast, *H. pulcherrimus* gut bending was sensitive to SB431542 until the prism stage. These data clearly indicate that gut bending is commonly dependent on a TGF-ß signal in sea urchins, but the timing of the response varies in different species.

Introduction

In bilaterians, gastrulation is required to form functional bodies composed of three germ layers: ectoderm, mesoderm, and endoderm; and Lewis Wolpert notes that gastrulation is the most important event in our lives (Lewis 2008). In the process of gastrulation in deuterostomes, the invagination forms a blastopore, generally a future anus, and the mouth opens later on the opposite side of the body. The position of the mouth in some deuterostomes is independent of gut formation because the stomodeum can be formed within the ventral ectoderm by itself without any endomesodermal structures in those animals (e.g., Wikramanayake & Klein 1997). In most vertebrates, the invaginated gut is extended toward the anterior at the ventral side of the body and fuses to the ventral ectoderm to open the mouth around the base of the future head

region. Because the gut in most vertebrates is at the relatively ventral side of the body from the beginning of invagination, only the extension toward the anterior is required to make "ventral" structures. However, in some deuterostomes, such as in sea urchins, that have a large blastocoel, the gut is initially extended toward the anterior in the middle axis of the body, and then, the tip of the gut has to bend toward the ventral side to form the "ventral" gut.

Gastrulation of sea urchin embryos is composed of primary and secondary invaginations. The primary invagination is driven by the apical constriction of the vegetal plate cells. The highly dense actin bundle at the apical side of vegetal plate cells produces the force to constrict the cell surface and unbalance the area of the cell surface between the apical and basal sides; the apical surface is smaller than that of the basal side; therefore, the vegetal plate is kinked into the blastocoel (reviewed in Kominami & Takata 2004). The secondary invagination leads to the elongation of the gut, which is managed with the pulling force by secondary mesenchyme cells and with conversion extension (Kominami & Takata 2004). Although these two steps of gastrulation are well studied, the mechanism of how the invaginated gut is fused to stomodeum to form the open mouth has not been well described. During the early gastrula, the gut elongates straight toward the anterior end of the body, but the tip of the gut reaches to the stomodeum located at the ventral ectoderm at the end of gastrulation; thus, the gut bends toward the ventral side during the process of gastrulation (Fig. 1). This phenomenon is conserved among some sea urchin species, at least in *Hemicentrotus pulcherrimus* and *Temnopleurus reevesii*, on which we focus in this paper. Because the gut in sea urchin embryos never bends in the wrong direction, such as to the dorsal side, the ventral ectoderm is expected to attract gut cells to proceed with the extension toward the mouth region. The dorsal-ventral patterning of the endomesoderm is regulated by TGF-ß superfamily members, such as Nodal and BMP2/4, in sea urchin embryos (Duboc et al. 2010), suggesting that the ventral attractant is among these factors. However, to date, no evidence indicates that TGF-ß factors are involved in the morphogenetic regulation of gut bending.

In Japanese developmental biology using sea urchins, *H. pulcherrimus* has been the prominent model organism for decades. In 2015, however, our group reported that *T. reevesii* could be another model sea urchin that can be used in developmental biology because of its rapid development, tolerance of high temperature and high

transparency (Yaguchi et al. 2015). In fact, *T. reevesii* is more beneficial for observing neurogenesis than *H. pulcherrimus*, which has a relatively longer developmental time to reach the neurogenic larval stages. Thus, because of the mutual compensation for their disadvantages and benefits, we use these two sea urchins in laboratory experiments to demonstrate the biological mechanisms that are shared beyond the differences in species. Here, with the advantage of the availability of the embryos of the two sea urchin species, we show that regulation by TGF-ß signals is the common mechanism for gut bending in sea urchin embryos.

Materials and Methods

Animals and embryo culture

Adult sea urchins *Hemicentrotus pulcherrimus* and *Temnopleurus reevesii* were collected around the Shimoda Marine Research Center (University of Tsukuba, Shizuoka, Japan) and Marine and Coastal Research Center (Ochanomizu University, Chiba, Japan). The gametes were collected by intrablastocoelic injection of 0.5 M KCl. The embryos of *H. pulcherrimus* and *T. reevesii* were incubated at 15˚C and 22˚C, respectively, and cultured in glass beakers or plastic dishes filled with filtered natural seawater (FSW) containing 50 µg/ml of kanamycin (Nacalai, Kyoto, Japan). In FSW, the final concentrations were 5.0 µM and 0.5 mM for SB431542 (Merck, Darmstadt, Germany) and $NiCl_2$, respectively. For the negative control of SB431542, we added the same volume of dimethyl sulfoxide (DMSO: Merck) into FSW. The timing of the application of these reagents is described in the text.

Cloning of TGF-ß family genes

Full-length of Nodal (LC369130), Lefty (LC369131), Bmp2/4 (LC369132) and Chordin (LC369133) cDNA were obrained from *Temnopleurus reevesii* cDNA by PCR using KOD FX DNA Polymerase (TOYOBO, Tokyo, Japan). Based on *T. reevesii* transcriptome sequence, the detail of which will be published elsewhere, the following primers were designed and used:

Tr-Nodal-F1: 5'-TCGATTATCGATATGCATCGTTTAGCCGAC-3' (underline shows ClaI site),

Tr-Nodal-R1: 5'-GTGATTCTCGAGGCGGTATGGTATTCGAAC-3' (underline shows XhoI site),

Tr-Lefty-F1: 5'-TCGATTGGATCCATGGAATTATCACTCGGC-3' (underline shows BamHI site),
Tr-Lefty-R1: 5'-GTGATTCTCGAGCGCCATGCATCCGCAATC-3' (underline shows XhoI site),
Tr-Bmp2/4-F1: 5'-TCGATTGAATTCATGGTTACCACCACACAC-3' (underline shows EcoRI site),
Tr-Bmp2/4-R1: 5'-GTGATTCTCGAGCTACCGGCACCCACAGCC-3' (underline shows XhoI site),
Tr-Chordin-F1: 5'-CATCGATTCGAATTCATGTATCGTGCTGTG-3' (underline shows EcoRI site),
Tr-Chordin-R1: 5'-TTCTAGAGGCTCGAGTTACGAGAGCTTCTC-3' (underline shows XhoI site).
Obtained cDNA were inserted into the pCS2+ vector and used for the following experiments.

Microinjection, whole-mount *in situ* hybridization and immunohistochemistry

Detailed methods for microinjection, whole-mount *in situ* hybridization, and immunohistochemistry are previously described (Yaguchi et al. 2016). The microinjection reagent was modified from 24% glycerol-DW to 24% glycerol-HK buffer (40 mM HEPES, pH 8.0, 120 mM KCl) for *H. pulcherrimus*, and glycerol was removed from the injection reagent for *T. reevesii*. The concentration and the sequence of Nodal morpholinos were as follow:
HpNodal-MO1 (300 μM), 5'-AGATCCGATGAACGATGCATGGTTA-3' (Yaguchi et al. 2010);
TrNodal-MO1 (380 μM), 5'-ATGCATGGTTAAAAGTCCGTAAAGT-3'.
Anti-serotonin (Sigma-Aldrich, St. Louis, MO, USA), anti-phosphorylated-Smad1/5/8 (pSmad1/5/8; Cell Signaling Technology, Danvers, MA, USA) and anti-pSmad2/3 (Abcam, Eugene, OR, USA) antibodies were diluted to 1/2,000, 1/1,000 and 1/100, respectively.

Quantitative polymerase chain reaction (qPCR)

qPCR was performed as previously described (Yaguchi, 2010, Ransick 2004) with some modeification. Total RNA from *T. reevesii* embryos were purified using ISOGEN

(Nippon Gene) and cDNA was synthesized with the reverse transcriptase SuperScript □ (Thermo Fischer Scientific). GoTaq qPCR Master Mix (Promega) was used for PCR with a Thermal Cycler Dice Real Time system (Takara). The primer sets used for QPCR are the followings:

Mitochondrial COI RNA-qF1: 5'- CCGCATTCTTGCTCCTTCTT -3',
Mitochondrial COI RNA-qR1: 5'- TGCTGGGTCGAAGAAAGTTG -3',
Nodal-qF2: 5'- GCA TCG TTT AGC CGA CAT CT -3',
Nodal-qR2: 5'- GGT CGA TGA TTT CGA CTC GT -3',
Lefty-qF2: 5'- GCA TTC GTC GTG CAT ACA TC-3',
Lefty-qR2: 5'- GAG TTC GGC CAT GAT GAT CT-3',
BMP2/4-qF1: 5'- CTT GTA TGC TGC GTT GTC GT-3',
BMP2/4-qR1: 5'- GAT CGC CCT CGT TAT GGT TA-3',
Chordin-qF1: 5'- ACA ACC TTG AGG ACG AAT GG-3', and
Chordin-qR1: 5'- CCA GCA GGA CAC CTT CAA AT-3'.

Relative amount of each mRNA were normalized with mitochondrial COI Ct values.

Results and Discussion

Temnopleurus reevesii embryos can be a comparative sea urchin model for studying the formation of dorsal-ventral polarity.

Based on previous works using four different sea urchin species, *Strongylocentrotus purpuratus*, *Paracentrotus lividus*, *Lytechinus variegatus*, and *H. pulcherrimus*, the dorsal-ventral axis formation is regulated by the combinational functions of Nodal, Lefty, BMP2/4, and Chordin, which are all expressed at the ventral ectoderm during early embryogenesis of sea urchins (Duboc et al. 2004; Nam et al. 2007; Coffman et al. 2004; Bradham et al. 2009; Yaguchi et al. 2016; Flowers et al. 2004). This observation suggests that embryos of *T. reevesii* also use the same system to establish the dorsal-ventral polarity because of the similar shapes of the embryonic/larval body. However, expressions of these four genes have not been reported in this species; therefore, the expression and function of these genes during embryogenesis required initial verification. To investigate the spatial expression patterns of these 4 TGF-ß members, we performed *in situ* hybridization analyses using early developmental stage embryos of *T. reevesii* from 8 to 18 h with 2 h intervals.

nodal was expressed at one side of 8 h embryos, with the expression continuing until at least 18 h (Fig. 2), and based on previous reports using other sea urchin species (Duboc et al. 2004; Saudemont et al. 2010), this expression was likely at the ventral ectoderm. The other three gene expression patterns were very similar to that of *nodal*, suggesting that these genes were also expressed at the ventral ectoderm (Fig. 2A). In fact, in 18 h embryos, in which the dorsal-ventral axis becomes prominent based on the position of PMC ventrolateral clusters (Duloquin et al. 2007), those genes are clearly expressed at ventral side. To confirm that the expression of these 4 genes was localized at the ventral ectoderm, we used $NiCl_2$ to ventralize sea urchin embryos (Hardin et al. 1992) and checked the expression of the genes. As expected, all of the genes were expressed radially to cover the entire ectoderm, except for the animal plate (anterior neuroectoderm) (Fig. 3I-P). Because the initiation of the expression of these genes remains uncertain (Duboc et al. 2004; Range et al. 2007), we attempted to perform *in situ* hybridization of TGF-ß members before 8 h, but the spatial expression patterns were not reproducible in individuals, and therefore, the precise expression patterns could not be determined. qPCR data supported this since each batch showed different temporal patterns with low amount of mRNAs (Fig. 2B). Based on *in situ* hybridization and qPCR,, we concluded that the gene was not maternally expressed, but by 8 h, the expression had begun.

To investigate whether Nodal was on top of the hierarchy of dorsal-ventral gene regulation of these 4 genes in *T. reevesii*, as in other sea urchins (e.g., Duboc et al. 2004), we investigated the gene expression patterns of the 4 genes in Nodal-deficient embryos. First, we blocked the Alk4/5/7-mediated TGF-ß signaling pathway using SB431542, which is a specific inhibitor of TGF/Activin type IB receptor (Inman et al. 2002). In SB431542-treated blastulae from 1 h post-fertilization, *nodal* was not expressed (Fig. 3Q, R), whereas control embryos expressed the gene normally (Fig. 3A, B). Expression of *lefty*, *bmp2/4*, and *chordin* was also not detected in the absence of Alk4/5/7 activity (Fig. 3C-H, S-X). Blocking the Alk4/5/7 receptor, SB431542 inhibited multiple TGF-ß family members, including Nodal and TGF-ß. Therefore, to focus on the specific function of Nodal, we employed a morpholino oligonucleotide against *nodal* (Nodal-MO) to block its translation and then determined the expression of the 4 genes. Several works have reported on the radialized morphology, significant decrease of ventrally expressed TGF-ß family genes, and radially distributed serotonergic

neurons in Nodal morphants in other species, such as in *H. pulcherrimus* (Fig. 4B, D, H, J, L)(Yaguchi et al. 2016), and a similar radialized phenotype, lack of the gene expressions (Fig. 3Y-f), and serotonergic neural patterns (Fig. 4A, C, G, I, K) were obtained in *T. reevesii* by injecting Nodal-MO; thus, the morpholino used in this experiment was supposed to be sufficiently specific to block translation of *nodal*, which showed that the Nodal-deficient effect was conserved beyond species. In Nodal morphants, *nodal* and the other 3 TGF-ß genes were not expressed in blastula stages (Fig. 3Y-f), which indicated that the expression of all 4 genes depended on Alk4/5/7 activity and the ligand was likely Nodal. Additionally, because Nodal morphants lost the expression of all of the genes, Nodal was at the top of the hierarchy of the signaling pathway involving these TGF-ß members, as reported in other species (Duboc et al. 2004; Saudemont et al. 2010). Collectively, *nodal*, *lefty*, *bmp2/4*, and *chordin* were expressed at the ventral ectoderm of *T. reevesii* embryos, and Nodal was required for their expression as in other sea urchin species (Duboc et al. 2004; Nam et al. 2007; Coffman et al. 2004; Bradham et al. 2009; Yaguchi et al. 2016; Flowers et al. 2004).

Although all of these 4 TGF-ß members are diffusing, notably, the expression site of their genes were well conserved among sea urchin species (Fig. 2), which indicates that the control system of the diffusion of Nodal, the top molecule in the regulatory hierarchy, is precisely organized in sea urchin groups (Nam et al. 2007; Duboc et al. 2008; Range et al. 2007). Nodal may diffuse only a few cell diameters in *S. purpuratus* embryos (Yaguchi et al. 2007), and Lefty, which can diffuse farther than Nodal, blocks the extra diffusion of Nodal at the future ciliary band region in *P. lividus* and *S. purpuratus* (Duboc et al. 2008; Yaguchi et al. 2010). Based on 4 TGF-ß RNA expression patterns localized only at the ventral region, it is suggested that Nodal-Lefty antagonism might function similarly in *T. reevesii* although we did not show the detailed expression patterns like using multi-color *in situ* hybridization. Therefore, the further analyses in future like the spatial expression profiling of 4 genes or the molecular interaction of both proteins might help us to understand Nodal-Lefty antagonism in *T. reevesii* embryos. According to the spatial expression data of *nodal*, we could not confidently conclude where the initial *nodal* was expressed. Because the results of previous reports using other species also remain debatable (Duboc et al. 2004; Range et al. 2007), spatial regulation might be unstable only at the beginning of gene expression, which could also be attributed to the faint amount of mRNA at the beginning and lack

of a protein detection tool, such as an anti-Nodal antibody, for sea urchin immunohistochemistry. Because of these points, when the first protein functions is difficult to determine. Alternatively, although anti-pSmad2/3, an intracellular mediator of the Nodal signal, can be one of the indicators of when and where the Nodal protein functions, unfortunately, the pSmad2/3 antibodies we used in this paper (Fig. 6) did not work on *T. reevesii* because of the difference in amino acid sequence at the C-terminal region. Thus, the understanding of the initial Nodal pathway functions in this sea urchin species must wait until useful antibody reagents are developed.

The expression and the functional data for TGF-ß family members in the early developmental stages of *T. reevesii* indicated that the gene regulatory network driving the dorsal-ventral axis formation was similar to that in other indirect developer sea urchin species. Combined with a previous report (Yaguchi et al. 2015), this result indicated that this species could be one of the model sea urchins in the study of developmental biology, particularly in analyzing axis formation during early embryogenesis. Currently, the identification of common features or biological phenomena and analyzing the detailed molecular mechanisms to show reproducible results is an important process. In this process, using different species in the same family is highly useful because when the same phenomena are identified or the same experimental results occur, the indication is that the sameness extends beyond the species differences and is likely a shared feature in the sea urchin family. For the examples above, the gut was straightly invaginated at the very beginning of the gastrula stage but bent toward the mouth in both *H. pulcherrimus* and *T. reevesii* by the prism stage (Fig. 1). The question in this case was what controls the morphogenetic behaviors of the sea urchin gut, which we could consider based on the results obtained from the experiments using two different species. With this strategy, a stronger conclusion could be reached than that when using a single species.

Alk4/5/7 signal is required for gut bending to the ventral side in the sea urchin embryo

To investigate the involvement of TGF-ß members in gut bending in sea urchin development, we first blocked translation of the dorsal-ventral master gene, *nodal*. However, because the morpholino injection interfered with the function of Nodal from the beginning, completely radialized embryos were produced in which the

ectoderm lost dorsal-ventral polarity and the gut elongated straight toward the anterior pole in both *T. reevesii* and *H. pulcherrimus*, as reported previously in other species (*cf.* Fig. 4C, D with A, B)(Duboc et al. 2004). These results were consistent with those of the Alk4/5/7 inhibitor SB431542 treatment, by which TGF-ß, including Nodal, activities were blocked at the reception level (Fig. 4E, F). Because these embryos completely lost the secondary body axis before invagination, we could not determine the effect of TGF-ß signals on gut bending. Therefore, we temporarily treated embryos with SB431542 to block the function of Alk4/5/7 during a certain period. Because the TGF-ß-dependent specification of dorsal-ventral ectoderm is completed by the gastrula stage (Duboc et al. 2005), we applied SB431542 from the early-gastrula until early pluteus stage. In SB431542-treated *T. reevesii*, in which the dorsal-ventral organization of the ectoderm was morphologically normal, the gut did not precisely bend toward the mouth region but did elongate to the animal pole region, whereas the gut bent to mouth region normally in control embryos (*cf.* Fig. 5F with A). Because the alkaline phosphatase activity in the mid- and hindgut was normal in SB431542-treated embryos and similar to that in the controls (Fig. 5B, G), the specification/differentiation of the gut cells was not severely affected, but gut bending was blocked by Alk4/5/7 inhibition (Fig. 5E, J). Similarly, in *H. pulcherrimus*, the gut elongated straightly toward the animal pole and not toward the mouth region with SB431542 treatment (Fig. 5C, D, H, I).

To quantify how much the gut bends in Alk4/5/7-deficient embryos and to estimate when the TGF-ß signal affects the gut, we measured the angle between the tip of the gut and anus in embryos treated with SB431542 at various stages (Fig. 5M). In *T. reevesii*, the data from two independent batches indicated that the gut did not precisely bend to the mouth when inhibition of the Alk4/5/7 signal began from the early gastrula to mid gastrula stages (Fig. 5K). After the late gastrula stage, the gut did not depend on the Alk4/5/7 signal for bending activity. By contrast, in *H. pulcherrimus*, the responsive period was longer than that in *T. reevesii* and occurred from the early gastrula to early prism stages (Fig. 5L), which might be attributed to the different styles of gastrulation between the species. The gut of *T. reevesii* elongates only halfway through the body (Yaguchi et al. 2015) and bends to the ventral side at the late gastrula stage, whereas the gut in *H. pulcherrimus* elongates straight to the animal pole at the late gastrula stage (e.g., Harada et al. 1995). Although we do not have information on what decides the gut

length during gastrulation in sea urchin development, the results of SB431542 treatment suggested that the Alk4/5/7 signal was required for gut morphogenetic behaviors until the timing immediately before bending in both species.

Although it has been previously reported that the dorsal-ventral pattern of the gut cell specification is dependent on TGF-ß signaling and that BMP molecules specify the dorsal characteristics of the gut (Duboc et al. 2010), whether Nodal/Activin/TGF-ß directly bind to the receptor on endodermal cells at SB431542-sensitive timing for gut bending remains unclear. For clarification, we attempted to detect phosphorylated-Smad2/3 (pSmad2/3) in gut cells during bending. At the late gastrula stage of *H. pulcherrimus*, a small amount of pSmad2/3 was in the nuclei at the ventral side of the tip of the gut and was abundant at dorsal side of the gut (Fig. 6A). However, because of the similarity of the amino acid sequences, the anti-pSmad3 antibody recognizes both phosphorylated C-termini of pSmad2/3 (…KQCSS*VS*; *expected phosphorylation site) and pSmad1/5/8 (…NPISS*VS*) (Yaguchi et al. 2007), and therefore, a definitive conclusion that the ventral faint signal was pSmad2/3 was difficult. To overcome this problem, we attempted to detect pSmad1/5/8 with an anti-pSmad1/5 antibody in the same stage embryos because this antibody only recognizes pSmad1/5/8 in *H. pulcherrimus* (Yaguchi et al. 2011). Comparing the patterns of pSmad2/3 with those of pSmad1/5/8, we did not detect any pSmad1/5/8 on the ventral side of the gut (Fig. 6B), indicating that pSmad2/3 was in the nuclei of ventral side of the bending gut. Importantly, pSmad2/3 in this region clearly disappeared with SB431542 treatment (Fig. 6C, D), supporting the idea that the direct Alk4/5/7 signal is required for gut bending toward the mouth region in *H. pulcherrimus*. At the dorsal side of the gut, whether pSmad2/3 was in the nuclei was unclear. Thus, we cannot discuss the involvement of Alk4/5/7 in the morphogenetic pathway at the dorsal side of the gut. Unfortunately, although the C-terminal region of Smad2/3 in *T. reevesii* (…KVCSS*MS*) is similar to that of *H. pulcherrimus*, the anti-Smad2/3 antibody did not cross-react between the species.

At the late gastrula stage, Nodal from the ventral ectoderm may bind to the tip of the gut and induce endodermal *nodal*, which is important for the later left-right asymmetric expression of *nodal* on the ectoderm (Molina et al. 2013; Bessodes et al. 2012). Thus, it is highly possible that the derivation of the nuclear pSmad2/3 at the tip of gut was from the ventral Nodal activity, although we could not completely eliminate

the possibility that Univin, TGF-ß and/or Activin was bound to the gut. In either case, the Alk4/5/7-pSmad2/3-mediated signaling pathway was required for gut bending. In sea urchin development, TGF-ß signals are certainly involved in morphogenesis. For examples, the Nodal and BMP2/4 pathways specify the ventral and dorsal ectoderm, respectively (Saudemont et al. 2010), and the cell-shape of the latter is much more squamous than that of the former. Although the mechanism by which those TGF-ß molecules regulate the cell-shape in sea urchin embryos remains unclear, the resultant ectoderm contributes to the formation of a pluteus shape in which the dorsal ectoderm occupies a wider area than that of the ventral ectoderm. Therefore, the Alk4/5/7 signal might mediate the cytoskeletal conformation to bend the gut to the mouth region. In fact, the actin filamentation of endodermal cells in vertebrates depends on a Nodal signal during gastrulation (Woo et al. 2012). Because Nodal-Alk4/5/7-Smad2/3 pathway induces *foxA* and *foxD* in the ventral endoderm (Duboc et al. 2010), these transcription factors might be suitable candidates for analyzing the mechanisms by which the TGF-ß-cytoskeleton pathway contributes to induce the morphological changes in endodermal cells of sea urchins. Direct regulation of the cytoskeleton by the Nodal pathway is also expected, and a detailed analysis of the relationship between the signaling pathway and the cytoskeletal regulation in the cells of the tip in the gut requires further study. By contrast, gut bending does not involve the BMP2/4-Smad1/5/8 pathway because the endoderm formation is normal in the absence of BMP2/4 activity (Yaguchi et al. 2010).

Conclusions

In this paper, we reached two conclusions that contribute to sea urchin developmental biology: 1) the embryos of *T. reevesii* are useful for studying axis specification/formation and 2) the Alk4/5/7 signal is required for gut bending toward the mouth. Our scientific claims are strengthened because these conclusions were based on the reproducible results of two different species, demonstrating that using multiple species in the lab can be a powerful tool. In Japanese sea urchin developmental biology, to date, *H. pulcherrimus* has been the most frequently used model organism. However, based on a previous study (Yaguchi et al. 2015) and this paper, we show that *T. reevesii* can be used as a routinely available model sea urchin in Japanese labs. Therefore, the similar behavior of gut bending was the focus in this additional species, and the

Alk4/5/7-Smad2/3 pathway was involved in the gut-bending step, which adds new information regarding morphogenesis of the sea urchin embryo. Because the invaginating gut undergoes conversion-extension, which is a process in which almost no cells divide (Kominami & Takata 2004), morphological changes of individual cells are important for the gut to bend. Thus, in future experiments, identification of the molecular linkage between TGF-ß signals and the regulation of the cytoskeleton in the endoderm of the sea urchin embryo is essential.

Acknowledgements

We thank Drs. J. Yaguchi, R. Burke and M. Kioyomoto for the essential reagents and technical advices. We thank Mrs. T. Sato, D. Shibata, M. Ooue, T. Kodaka, J. Takano, and M. Yamaguchi for collecting and keeping the adult sea urchins. This work is supported by Takeda Science Foundation and Kishimoto Foundation (Senri Life Science Foundation).

References

Bessodes, N. et al., 2012. Reciprocal Signaling between the Ectoderm and a Mesendodermal Left-Right Organizer Directs Left-Right Determination in the Sea Urchin Embryo. *PLoS Genetics*, 8(12).

Bradham, C. a et al., 2009. Chordin is required for neural but not axial development in sea urchin embryos. *Developmental biology*, 328(2), pp.221–33. Available at: http://www.pubmedcentral.nih.gov/articlerender.fcgi?artid=2700341&tool=pmcentrez&rendertype=abstract [Accessed October 8, 2013].

Coffman, J. a et al., 2004. Oral-aboral axis specification in the sea urchin embryo II. Mitochondrial distribution and redox state contribute to establishing polarity in Strongylocentrotus purpuratus. *Developmental biology*, 273(1), pp.160–71. Available at: http://www.ncbi.nlm.nih.gov/pubmed/15302605 [Accessed October 8, 2013].

Duboc, V. et al., 2005. Left-right asymmetry in the sea urchin embryo is regulated by nodal signaling on the right side. *Developmental cell*, 9(1), pp.147–58. Available at: http://www.ncbi.nlm.nih.gov/pubmed/15992548 [Accessed October 8, 2013].

Duboc, V. et al., 2008. Lefty acts as an essential modulator of Nodal activity during sea urchin oral-aboral axis formation. *Developmental biology*, 320(1), pp.49–59.

Available at: http://www.ncbi.nlm.nih.gov/pubmed/18582858 [Accessed October 8, 2013].

Duboc, V. et al., 2010. Nodal and BMP2/4 pattern the mesoderm and endoderm during development of the sea urchin embryo. *Development (Cambridge, England)*, 137(2), pp.223–35. Available at: http://www.ncbi.nlm.nih.gov/pubmed/20040489 [Accessed October 8, 2013].

Duboc, V. et al., 2004. Nodal and BMP2/4 signaling organizes the oral-aboral axis of the sea urchin embryo. *Developmental cell*, 6(3), pp.397–410. Available at: http://www.ncbi.nlm.nih.gov/pubmed/15030762.

Duloquin, L., Lhomond, G. & Gache, C., 2007. Localized VEGF signaling from ectoderm to mesenchyme cells controls morphogenesis of the sea urchin embryo skeleton. *Development (Cambridge, England)*, 134(12), pp.2293–2302.

Flowers, V.L. et al., 2004. Nodal/activin signaling establishes oral-aboral polarity in the early sea urchin embryo. *Developmental dynamics : an official publication of the American Association of Anatomists*, 231(4), pp.727–40. Available at: http://www.ncbi.nlm.nih.gov/pubmed/15517584 [Accessed October 8, 2013].

Harada, Y., Yasuo, H. & Satoh, N., 1995. A sea urchin homologue of the chordate Brachyury (T) gene is expressed in the secondary mesenchyme founder cells. *Development (Cambridge, England)*, 121(9), pp.2747–54. Available at: http://www.ncbi.nlm.nih.gov/pubmed/7555703.

Hardin, J. et al., 1992. Commitment along the dorsoventral axis of the sea urchin embryo is altered in response to NiCl 2. , 685, pp.671–685.

Inman, G.J. et al., 2002. SB-431542 Is a Potent and Specific Inhibitor of Transforming Growth Factor-beta Superfamily Type I Activin Receptor-Like Kinase (ALK) Receptors ALK4, ALK5, and ALK7. *Molecular Pharmacology*, 62(1), pp.65–74. Available at: http://molpharm.aspetjournals.org/cgi/doi/10.1124/mol.62.1.65.

Kominami, T. & Takata, H., 2004. Gastrulation in the sea urchin embryo: A model system for analyzing the morphogenesis of a monolayered epithelium. *Development Growth and Differentiation*, 46(4), pp.309–326.

Lewis, W., 2008. The Triumph of the Embryo. *Courier Corporation*.

Molina, M.D. et al., 2013. Nodal: Master And Commander Of The Dorsal-Ventral And Left-Right Axes In The Sea Urchin Embryo. *Current Opinion in Genetics and Development*, 23(4), pp.445–453.

Nam, J. et al., 2007. Cis-regulatory control of the nodal gene, initiator of the sea urchin oral ectoderm gene network. *Developmental biology*, 306(2), pp.860–9. Available at: http://www.pubmedcentral.nih.gov/articlerender.fcgi?artid=2063469&tool=pmcentrez&rendertype=abstract [Accessed October 8, 2013].

Range, R. et al., 2007. Cis-regulatory analysis of nodal and maternal control of dorsal-ventral axis formation by Univin, a TGF-beta related to Vg1. *Development (Cambridge, England)*, 134(20), pp.3649–64. Available at: http://www.ncbi.nlm.nih.gov/pubmed/17855430 [Accessed October 8, 2013].

Saudemont, A. et al., 2010. Ancestral regulatory circuits governing ectoderm patterning downstream of Nodal and BMP2/4 revealed by gene regulatory network analysis in an echinoderm. *PLoS genetics*, 6(12), p.e1001259. Available at: http://www.pubmedcentral.nih.gov/articlerender.fcgi?artid=3009687&tool=pmcentrez&rendertype=abstract [Accessed September 24, 2013].

Wikramanayake, a H. & Klein, W.H., 1997. Multiple signaling events specify ectoderm and pattern the oral-aboral axis in the sea urchin embryo. *Development (Cambridge, England)*, 124(1), pp.13–20. Available at: http://www.ncbi.nlm.nih.gov/pubmed/9006063.

Woo, S. et al., 2012. Nodal signaling regulates endodermal cell motility and actin dynamics via Rac1 and Prex1. *Journal of Cell Biology*, 198(5), pp.941–952.

Yaguchi, J. et al., 2016. Cooperative Wnt-Nodal Signals Regulate the Patterning of Anterior Neuroectoderm. *PLoS genetics*, 12(4), p.e1006001.

Yaguchi, S. et al., 2010. ankAT-1 is a novel gene mediating the apical tuft formation in the sea urchin embryo. *Developmental biology*, 348(1), pp.67–75. Available at: http://www.pubmedcentral.nih.gov/articlerender.fcgi?artid=2976814&tool=pmcentrez&rendertype=abstract [Accessed October 8, 2013].

Yaguchi, S. et al., 2015. Early development and neurogenesis of Temnopleurus reevesii. *Development Growth and Differentiation*, 57(3), pp.242–250.

Yaguchi, S. et al., 2011. Fez function is required to maintain the size of the animal plate in the sea urchin embryo. *Development (Cambridge, England)*, 138(19), pp.4233–43. Available at: http://www.pubmedcentral.nih.gov/articlerender.fcgi?artid=3171223&tool=pmcentrez&rendertype=abstract [Accessed October 8, 2013].

Yaguchi, S. et al., 2010. TGFβ signaling positions the ciliary band and patterns neurons in the sea urchin embryo. *Developmental biology*, 347(1), pp.71–81. Available at: http://www.pubmedcentral.nih.gov/articlerender.fcgi?artid=2950233&tool=pmcentrez&rendertype=abstract [Accessed October 8, 2013].

Yaguchi, S., Yaguchi, J. & Burke, R.D., 2007. Sp-Smad2/3 mediates patterning of neurogenic ectoderm by nodal in the sea urchin embryo. *Developmental biology*, 302(2), pp.494–503. Available at: http://www.ncbi.nlm.nih.gov/pubmed/17101124 [Accessed October 8, 2013].

Figure legends

Figure 1. Straightly invaginated gut bends toward the ventral side at the later stages in sea urchin embryos.

T. reevesii (A, C) and *H. pulcherrimus* (B, D) embryos at the gastrula stages. The gut initially invaginates straight toward the anterior end of the body, but bends toward the ventral side at later stages. Dashed lines, the outline of the gut; Arrows, the direction of the elongated gut; LV, Lateral views; MG, Mid gastrula; Pr, Prism larvae. Bar in (A) is 20 μm.

Figure 2. Gene expression patterns of the TGF-β members responsible for establishing dorsal-ventral axis in *T. reevesii*.

(A) Whole-mount *in situ* hybridizations detecting *nodal*, *lefty*, *bmp2/4*, and *chordin* in normal development, which are expressed at the one side of the embryo. AV, Anterior views; LV, Lateral views. Double-headed arrows indicate the ventral (V)-dorsal (D) axis. (B) Relative amount of the mRNA of TGF-ß members in 2 h, 6h, and 10 h sea urchin embryo.

Figure 3. TGF-ß members are expressed at the ventral ectoderm in *T. reevesii*.

Whole-mount *in situ* hybridizations detecting, *nodal*, *lefty*, *bmp2/4*, and *chordin* in control, SB431542-treated, Nodal-deficient, and $NiCl_2$-treated embryos of *T. reevesii*. (A-H) At the blastula stage, the four TGF-β members are expressed on one side of the ectoderm. (I-P) In embryos ventralized by $NiCl_2$ treatment from 30 minutes

post-fertilization, all TGF-ß genes were expressed in the entire ectoderm except for the anterior neuroectoderm. (Q-X) When Alk4/5/7 was blocked with SB431542 from 1 h post-fertilization, TGF-β expression was suppressed. (Y-f)Expression of TGF-β mRNA was absent in Nodal morphants. AV, Anterior views; LV, Lateral views; MB, Mesenchyme blastula.

Figure 4. Inhibiting the Nodal and/or Alk4/5/7 pathways produces embryos in which the dorsal-ventral axis is missing.

(A, B) Control (DMSO treated) embryos show the bending gut to the ventral ectoderm in *T. reevesii* and *H. pulcherrimus*. (C, D) Nodal morphants of *T. reevesii* and *H. pulcherrimus* lose the dorsal-ventral axis, and the gut elongates straight to the anterior pole. Insets indicate the anterior views. (E, F) SB431542 treatment from 1 h post-fertilization to prism larvae in both species impairs the dorsal-ventral axis, in addition to that of Nodal morphants. (G, H) The serotonergic neurons in control (glycerol-injected) or embryos of *T. reevesii* and *H. pulcherrimus*. Serotonin-positive cells align straightly along the left-right axis in the anterior neuroectoderm. (I-L) Radially distributed serotoneric neurons in Nodal morphants of *T. reevesii* and *H. pulcherrimus*. Dashed lines, the outline of the gut; Arrows, the direction of the elongated gut; LV, lateral-view; AV, anterior-view.

Figure 5. Alk4/5/7-mediated signal is required for gut bending toward the ventral side in sea urchin.

The gut bends toward the ventral side and forms an open mouth in the control pluteus (A-E), but extends toward the anterior end of the body in SB431542-treated embryos (F-J). (A, B, F, G) *T. reevesii* and (C, D, H, I) *H. pulcherrimus*. (A, C, F, H) Bright field images. (B, D, G, I) Alkaline phosphatase activity in the mid- and hindgut. (E, J) Schematic images of control and SB431542-treated embryos. Dashed lines, the outline of the gut; White arrowheads, the position of the stomodeum; Red arrows, the direction of the elongated gut. Angle of curvature of the gut in *T. reevesii* (K) and in *H. pulcherrimus* (L). (M) The image shows how the curvature of the gut was measured with the angle (θ). Embryos were treated with SB431542 starting at different stages, and the curvature of the gut was measured at the early pluteus larvae. Each bar indicates the average angle from 10 individuals in the same batch with mean ± SEM. EG, Early

gastrula; MG, Mid gastrula; LG, Late gastrula; Pr, Prism; EPr, Early prism; LPr, Late prism. DMSO indicates the negative control.

Figure 6. Alk4/5/7-pSmad2/3 pathway functions at the ventral side of the tip of the gut during gastrulation in *H. pulcherrimus*.

Phosphorylated-Smad2/3 (pSmad2/3) is at the ventral side of the tip of the gut in control (DMSO-treated) (A) but not SB431542-treated embryos (C). pSmad1/5/8 is only at the dorsal side in either control (B) or SB431542-treated embryos (D). Dashed-line square areas in (A, B, C, D) are magnified in (A', B', C', D'), respectively. Dashed lines outline the gut in (A', B', C', D'). (A'', B'', C'', D'') Schematic images of pSmad2/3 and pSmad1/5/8 patterns in the gut of control and SB431542-treated embryos. Because of the similarity of the amino acid sequences, the anti-pSmad3 antibody recognizes both phosphorylated C-termini of pSmad2/3 and pSmad1/5/8. LV, Lateral views; Hp, *H. pulcherrimus*; LG, Late gastrula. Numbers in (A', B', C', D') = Number of embryos that showed pSmad2/3 or pSmad1/5/8 in gut ventral cells/Number of total embryos observed.

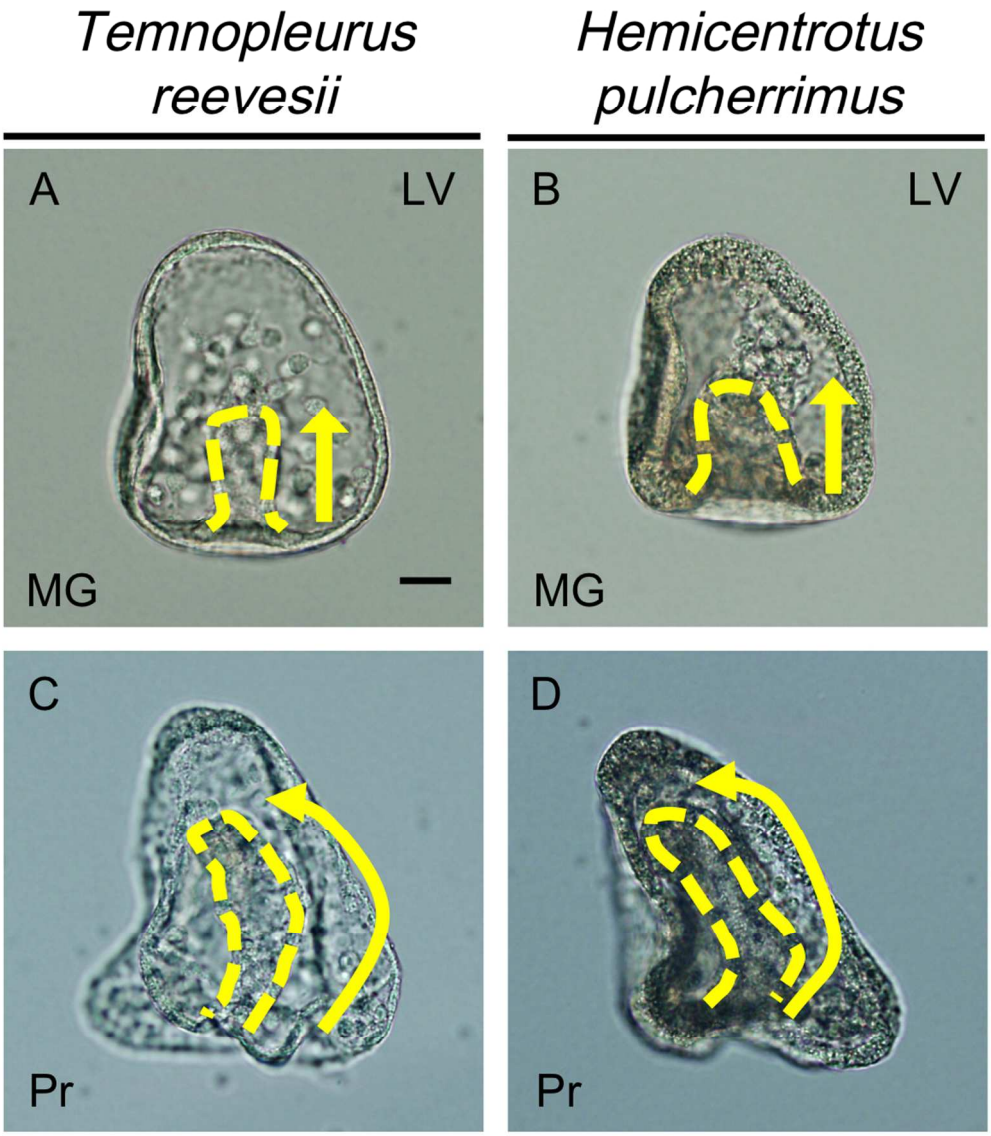

Figure_1

413x468mm (72 x 72 DPI)

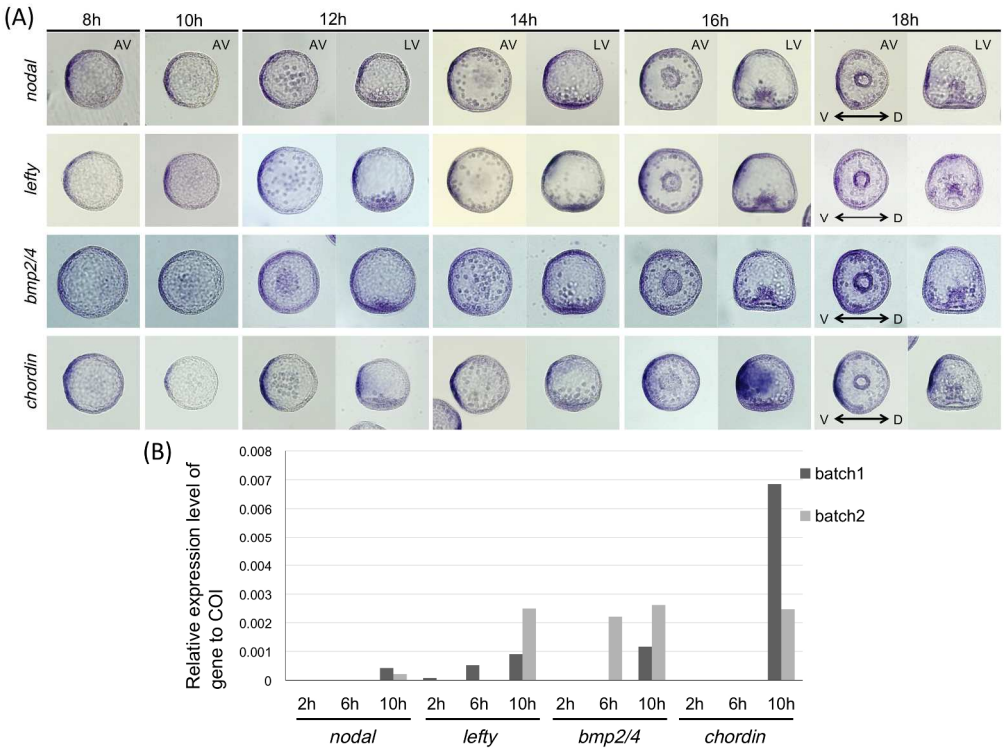

Figure_2

999x746mm (72 x 72 DPI)

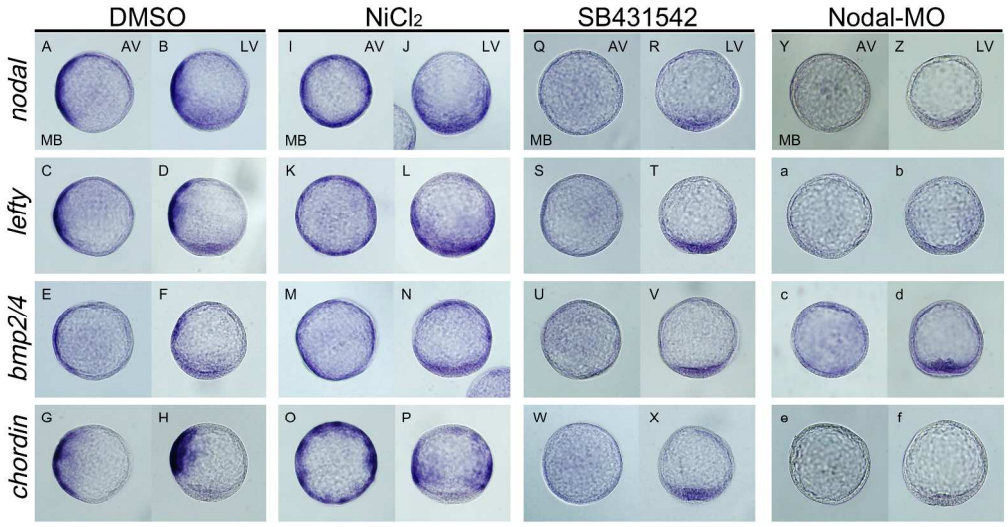

Figure_3

1012x525mm (72 x 72 DPI)

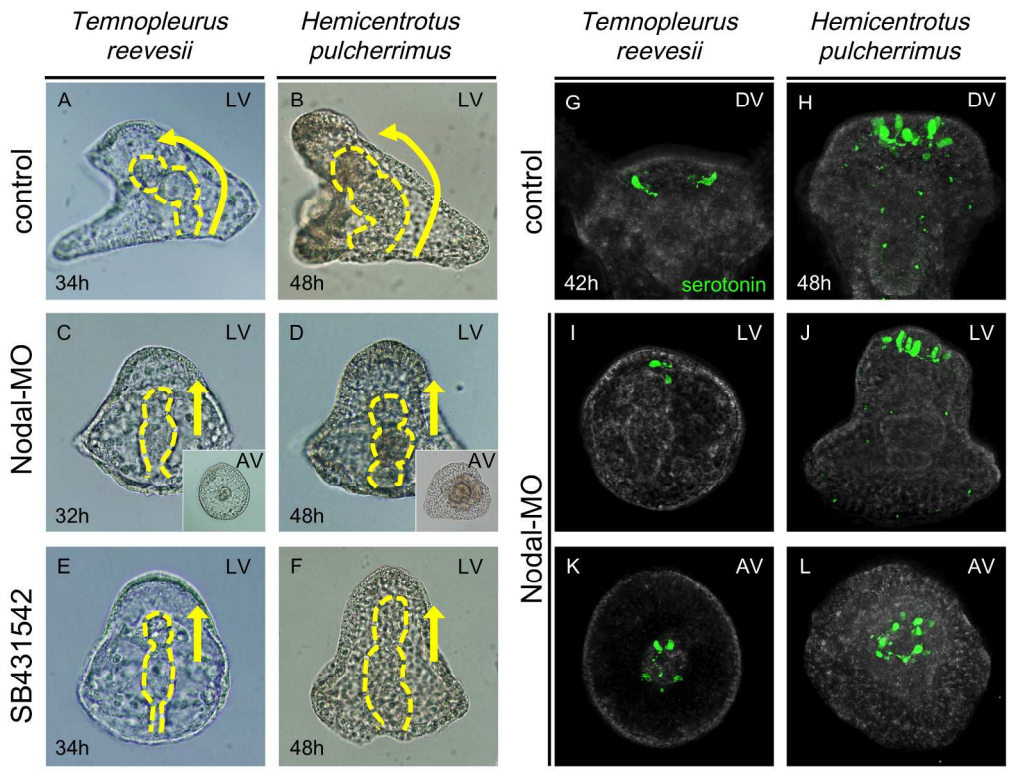

Figure_4

905x689mm (72 x 72 DPI)

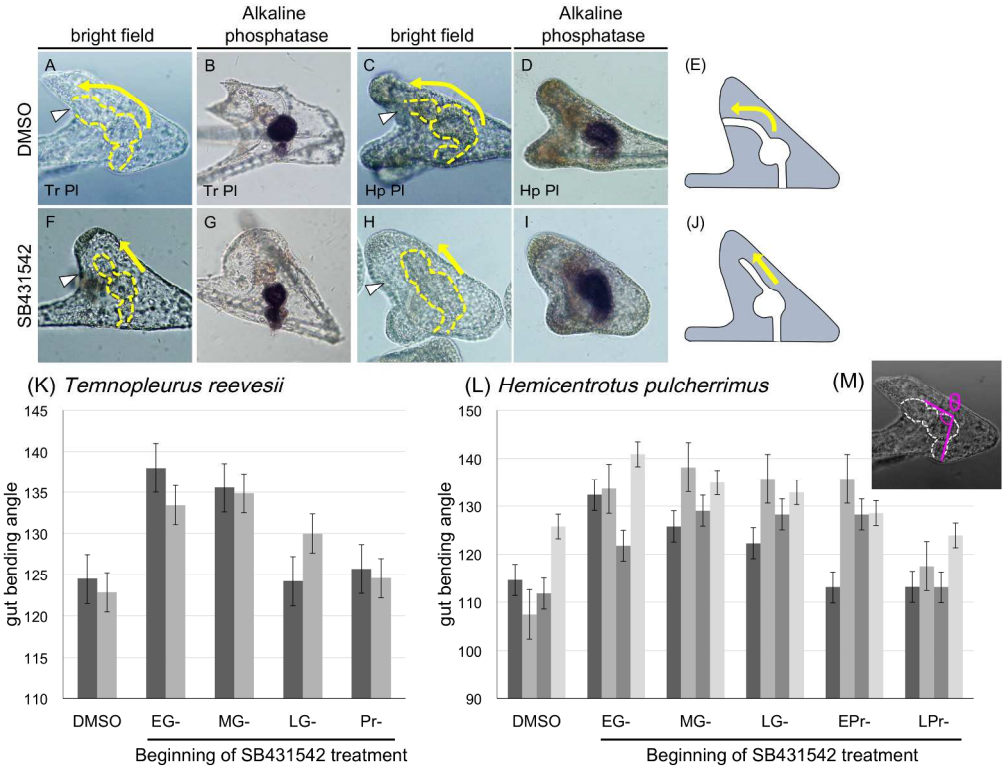

Figure_5

1030x785mm (72 x 72 DPI)

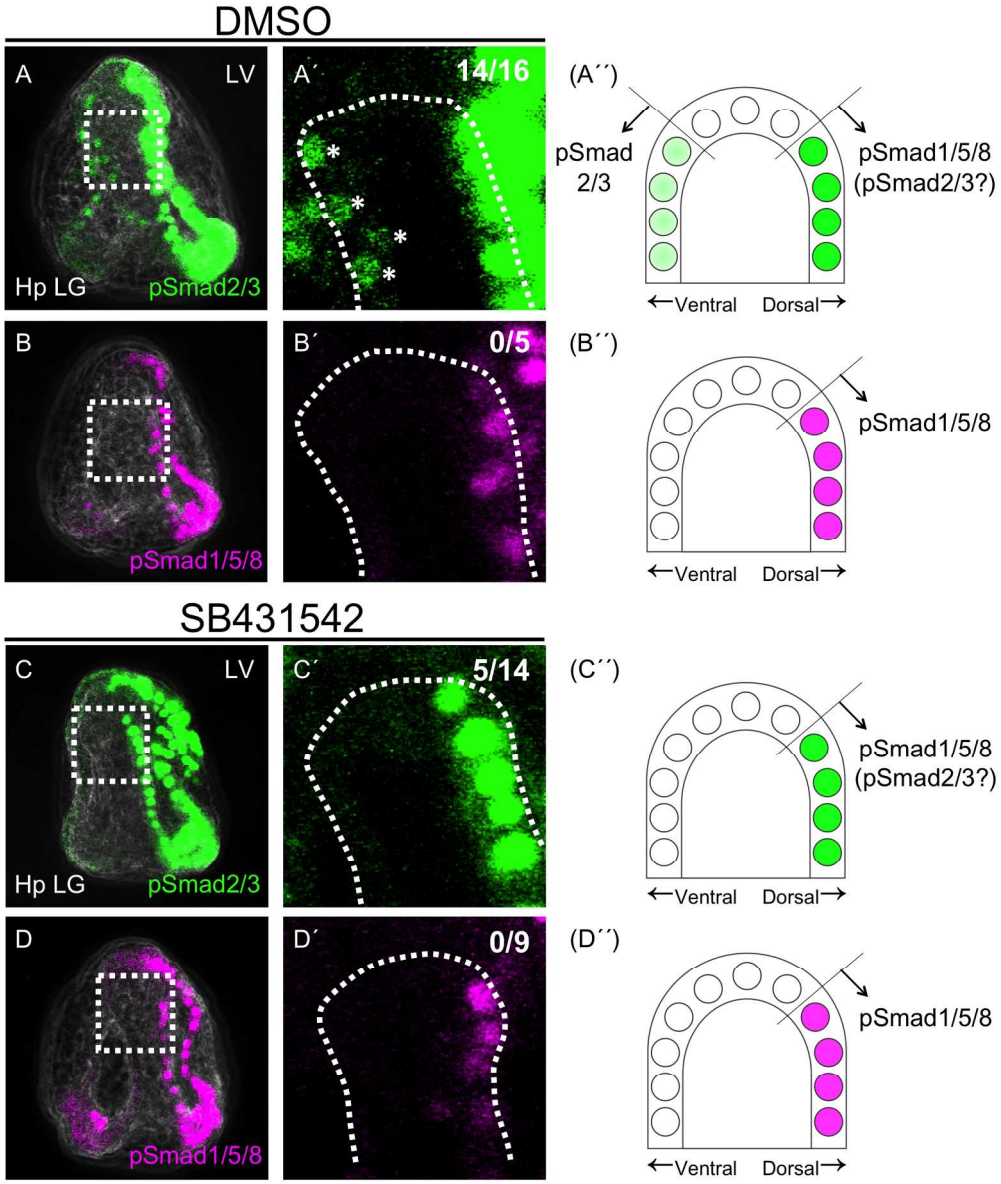

Figure_6

755x889mm (72 x 72 DPI)